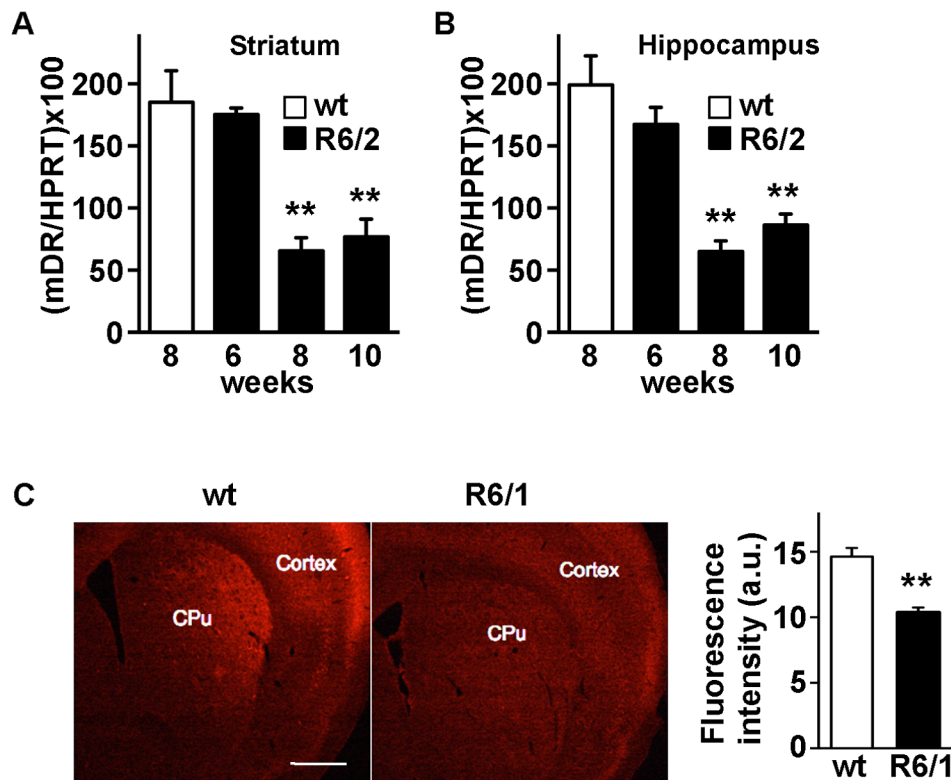
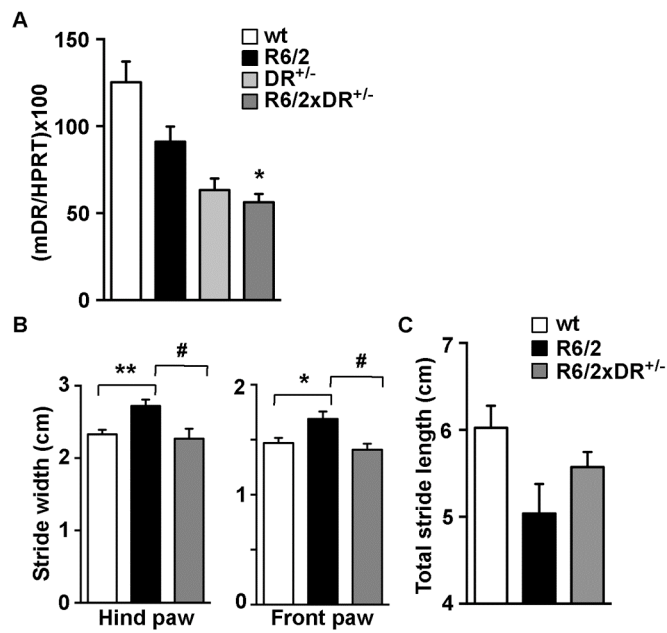


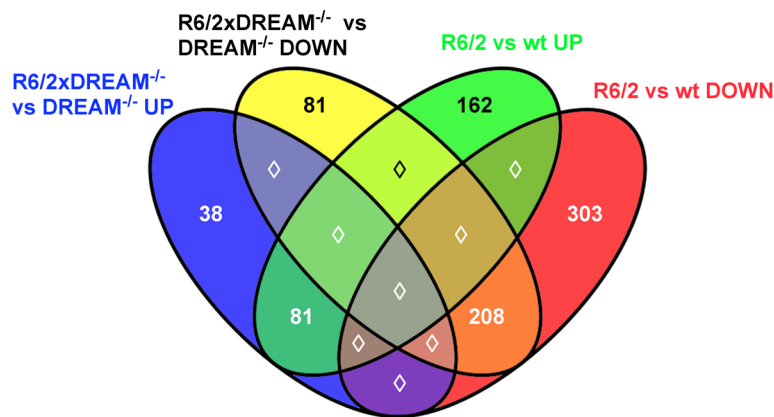
Supplemental Figures



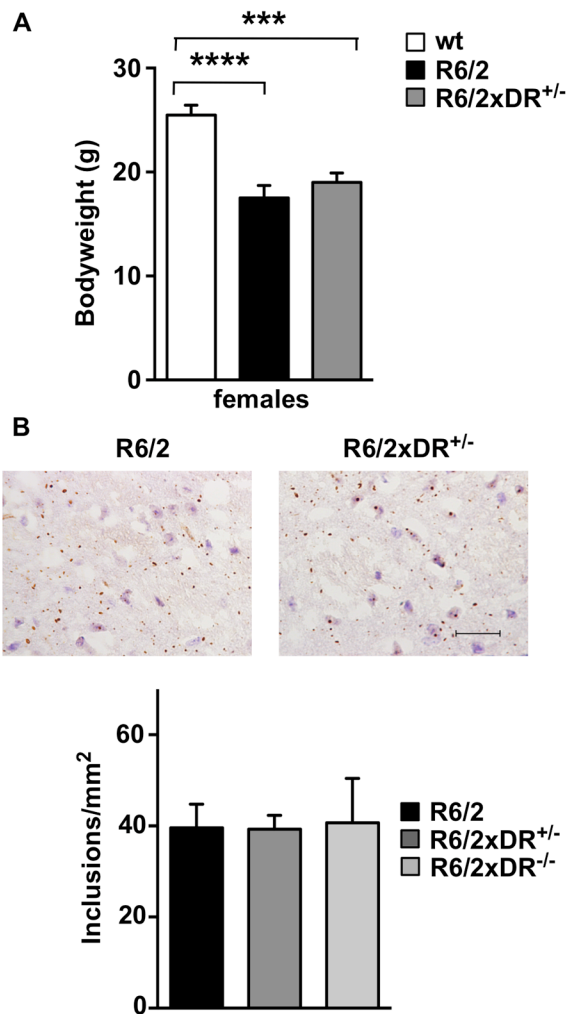
Supplemental Figure 1. Changes in DREAM expression in the brain in R6 mouse models. (A, B) Real-time qPCR analysis of DREAM mRNA levels in striatum (A) and hippocampus (B) of 6- to 10-week-old R6/2 and 8-week-old wild-type mice. DREAM mRNA expression in wild type mice was stable between 6 to 10 weeks after birth. Values are normalized relative to HPRT mRNA levels. Six mice were analyzed in each group in two independent experiments. Significant differences compared to wt were identified using one-way ANOVA with Dunnett's multiple comparisons test. ** $P < 0.01$. (C) Immunohistochemistry with anti-DREAM antibody in coronal sections, showing caudate putamen (CPu) and cortex from 7 week-old R6/1 mice. Fluorescence intensity (mean \pm SEM) of DREAM in CPu was lower in R6/1 mice than in wild-type littermates (unpaired two-tailed Student's t -test, $n = 6$, ** $P < 0.01$). Bar = 500 μm .



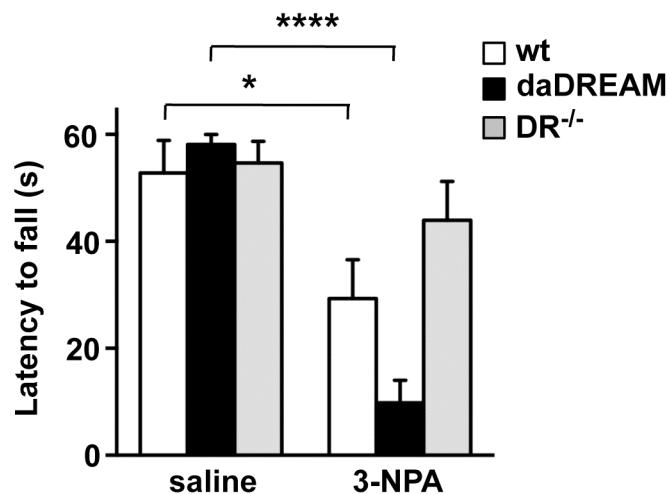
Supplemental Figure 2. Analysis of DREAM levels and motor coordination in R6/2xDREAM^{+/-} mice. (A) Quantitative real-time PCR analysis of endogenous DREAM mRNA levels in the striatum of 8-week-old mice of the indicated genotypes. Values are normalized to HPRT mRNA content. Six mice were analyzed in each group in 2 independent experiments. A significant difference was found between R6/2xDREAM^{+/-} vs R6/2 mice. * $P = 0.0164$ (unpaired two-tailed Student's t -test). (B and C) Motor coordination analysis using the footprint test. (B) Stride width (mean \pm SEM) of hind and front paws of 16-week-old mice of the indicated genotypes are shown ($n = 12$ per group). * $P < 0.05$, ** $P < 0.01$ vs wt, # $P < 0.05$ vs R6/2 (one-way ANOVA, followed by Tukey's test). (C) Stride length (mean \pm SEM) of 16-week-old mice of the indicated genotypes are shown ($n = 12$ per group). Reduction in stride length in R6/2 mice and recovery in R6/2xDREAM^{+/-} were noticeable, though did not reach statistical significance.



Supplemental Figure 3. Genome-wide analysis of R6/2xDREAM^{+/-} striatum. Striatal gene expression in wild type, R6/2, R6/2xDREAM^{+/-} and DREAM^{+/-} mice was compared using cDNA microarrays. The results (Gene Expression Omnibus accession number GSE48104) showed a general reduction in the extent of transcriptomic changes in R6/2xDREAM^{+/-} compared to R6/2 striatum. The Venn diagram shows the combinations of up- and downregulated genes for wild-type vs R6/2 and DREAM^{+/-} vs R6/2xDREAM^{+/-}. For each comparison, genes with FDR < 0.005 (Benjamini-Hochberg correction for multiple comparison) were considered to be differentially expressed. Approximately, 60% of the genes downregulated in R6/2 striatum (303 of 511) were expressed normally in R6/2xDREAM^{+/-} striatum, which did not differ from expression in DREAM^{+/-} or wild-type mouse striatum (see also Supplementary Table 2). More than 75% of genes upregulated in R6/2 striatum (162 of 211) was not modified in R6/2xDREAM^{+/-} striatum (see also Supplementary Table 3).



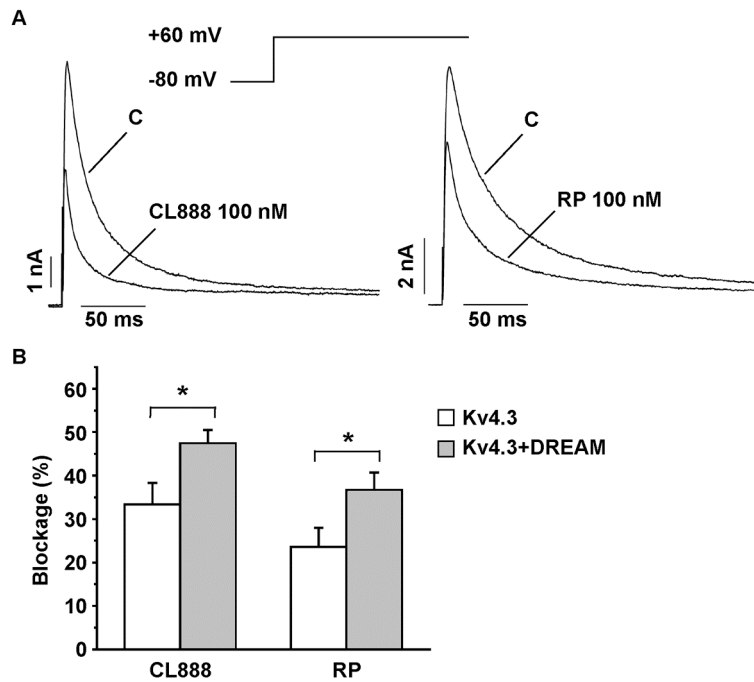
Supplemental Figure 4. Analysis of body weight and mHtt inclusions in R6/2xDREAM^{+/-} mice. (A) Body weight of 16-week-old female mice of the indicated genotypes. Data (mean \pm SEM) were analyzed by one-way ANOVA followed by Tukey's multiple comparisons test and showed no significant change in phenotype by crossing R6/2 and DREAM^{-/-} mice. Wild type mouse (wt, $n = 12$) body weight differed significantly from that of R6/2 ($n = 10$) and R6/2xDR^{+/-} mice ($n = 12$), *** $P < 0.001$. (B) Huntingtin immunoreactive inclusions in striatal tissue from mice of indicated genotypes. Bar = 50 μ m. Bottom, quantification of Htt-positive inclusions in the distinct genotypes shown as positive inclusions per mm².



Supplemental Figure 5. Differential response to 3-NP depending on DREAM levels.

Latency to fall in the rotarod test was analyzed in mice of the indicated genotypes ($n = 4-8$) that received four injections of saline or 3-NPA within 48 h. Administration of 3-NPA to wild type mice induced progressive loss of motor coordination in the rotarod test, which was statistically significant after the last 3-NPA injection. In transgenic mice that overexpressed a dominant active mutant DREAM (daDREAM), reduced latency to fall was observed after the first injection and was highly significant after the last injection. In DREAM^{-/-} mice, however, no effect was observed at any time after 3-NPA treatment, suggesting that the lack of DREAM is neuroprotective in this chemical HD model. The effect of treatment between mice of different genotypes was analyzed by two-way ANOVA followed by Sidak's test.

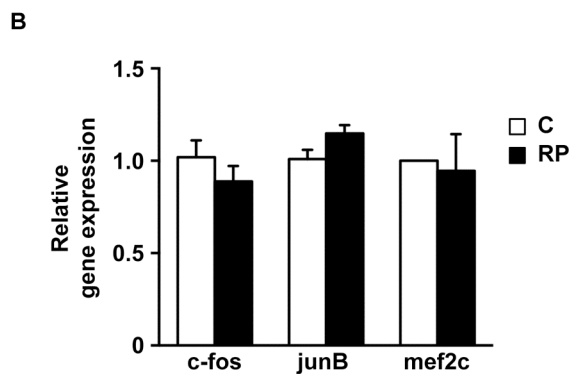
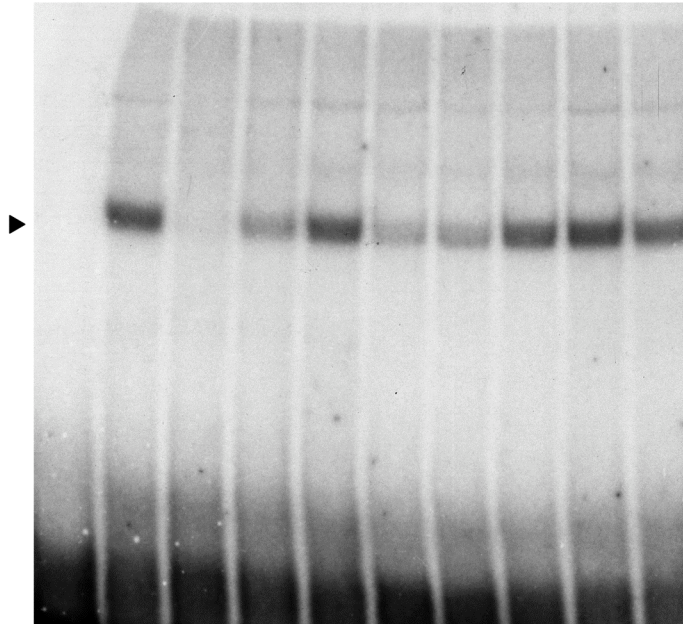
* $P < 0.05$, **** $P < 0.0001$.



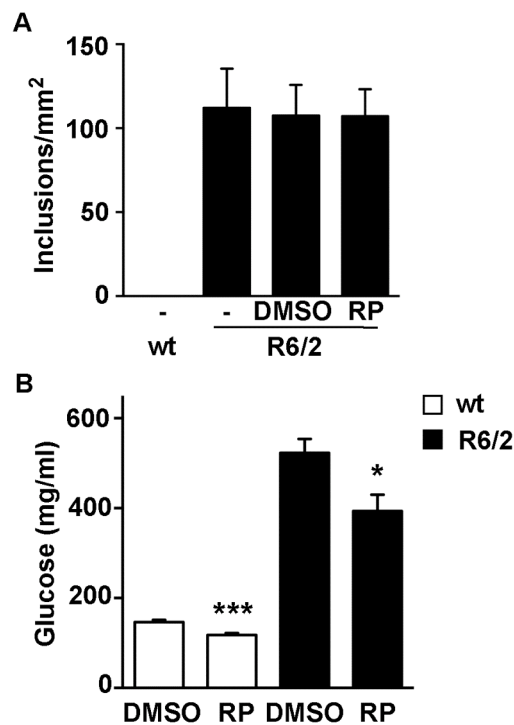
Supplemental Figure 6. Effect of CL-888 and repaglinide on Kv4.3 and Kv4.3+DREAM channels. (A) Representative Kv4.3 currents recorded in CHO cells transiently transfected with the Kv4.3 expression plasmid alone. Current traces were obtained after depolarization to +60 mV from a holding potential of -80 mV. Currents were recorded in control conditions and after perfusion with 100 nM CL-888 (left) or 100 nM repaglinide (RP, right). (B) Graph showing the degree of blockage produced by CL-888 and repaglinide at 100 nM on Kv4.3 and Kv4.3+DREAM. Note that both compounds block to a higher extent Kv4.3 currents in the presence of DREAM. Data represent mean \pm SEM of 3 to 9 experiments.

A

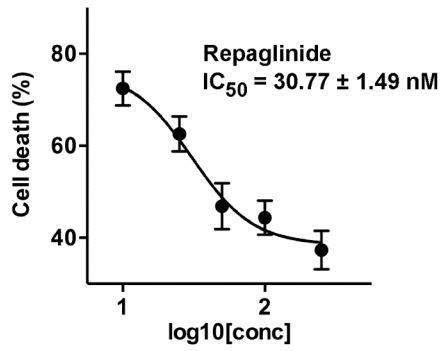
DREAM	-	+	+	+	+	+	+	+	+	+
Cold probe	-	-	10x	1x	-	-	-	-	-	-
Sp1	-	-	-	-	10x	-	-	-	-	-
DMSO	-	-	-	-	-	+	-	-	-	-
RP, μ M	-	-	-	-	-	-	10^3	10^2	10	1



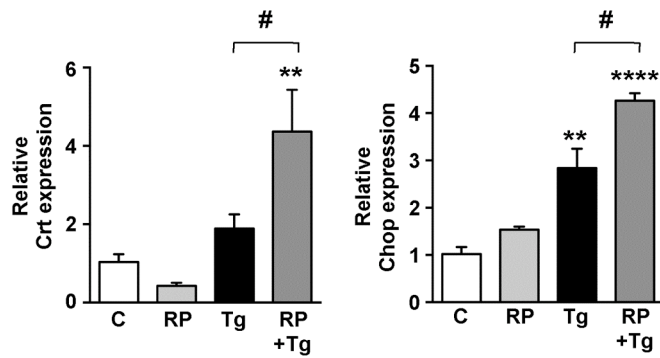
Supplemental Figure 7. Repaglinide does not modify binding of DREAM to DRE sites. (A) Band-shift analysis of recombinant DREAM binding to a DRE probe. Competition with cold DRE probe (lanes 3 and 4) and no effect with unrelated cold Sp1 probe (lane 5). Repaglinide (RP) (up to 0.1 mM) did not affect DREAM binding to the probe (lanes 8 to 10). Migration of the free DRE probe (lane 1). Non-specific competition by 1 μ l DMSO (100%) (lane 6) or with 1 mM RP in 100% DMSO (lane 7). Arrowhead, retarded band. (B) Real-time qPCR analysis of basal mRNA levels of DREAM target genes in N2a neuroblastoma cells treated with repaglinide (RP). Values are normalized to HPRT mRNA levels and expressed relative to control untreated cells (C). One-way ANOVA showed no statistically difference between groups.



Supplemental Figure 8. Analysis of mHtt inclusions and glucose levels in R6/2 mice after repaglinide administration. (A) Quantification of Htt immunoreactive inclusions in striatal tissue from mice of indicated genotypes that were untreated (-) or received vehicle (DMSO) or repaglinide (4 μ g/ml, RP) in drinking water. Quantification is shown as positive inclusions per mm². (B) Glucose levels in blood from wild type (wt) or R6/2 mice that received vehicle (DMSO) or repaglinide (4 μ g/ml, RP) in drinking water. Glucose levels were assessed 90 min after access to food following a 12-h fast. *** $P < 0.001$ * $P < 0.05$ (n = 11-17, unpaired, two-tailed t -test).

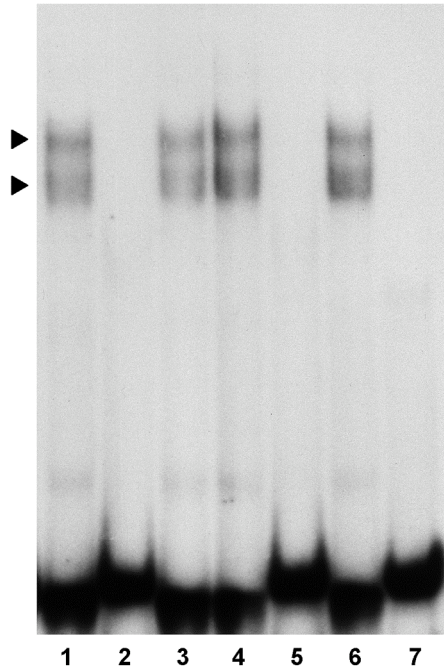


Supplemental Figure 9. Concentration curve for the inhibitory effect of repaglinide on the disruption of the mitochondrial membrane potential induced by H₂O₂. STHdhQ^{7/7} cells were pretreated with increasing concentrations of repaglinide for 30 min and then stimulated with H₂O₂ (10 μM, 3 h). Data from 4 independent experiments in triplicates were analyzed. Healthy (red) and damaged (green) cells from three separate fields were counted from each culture plate. A four-parameter (variable slope) non-linear curve fitting resulted in an IC_{50} of 30.77 ± 1.49 nM for repaglinide.

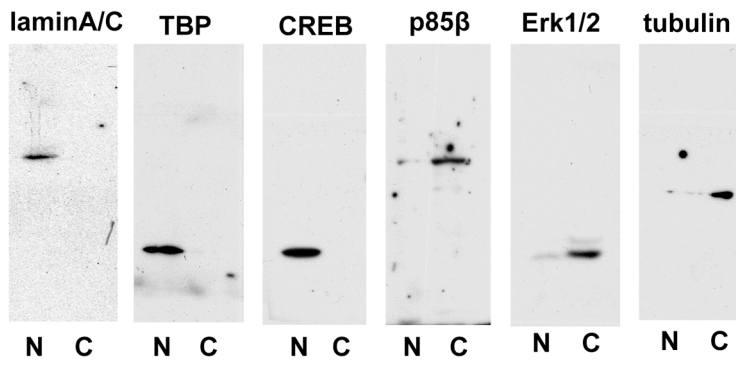


Supplemental Figure 10. Real-time qPCR analysis of calreticulin (Crt) and Chop mRNAs. STHdhQ^{7/7} cells, alone or pretreated with repaglinide (RP, 200 nM, 1 h), were stimulated with thapsigargin (Tg, 200 nM, 7 h). Values are normalized to HPRT mRNA content, and correspond to 3 independent experiments in triplicate. Significant differences were identified using one-way ANOVA with Bonferroni multiple comparison test ** $P < 0.01$ and **** $P < 0.0001$, compared to control. # $P < 0.05$ for thapsigargin-stimulated cells, with or without repaglinide pretreatment.

ATF6-bZIP	+	+	+	+	-	+	-
Cold probe	-	+	-	-	-	-	-
DREAM	-	-	+	+	+	-	-
RP	-	-	-	+	-	+	-



Supplemental Figure 11. Band-shift analysis of bZIP-ATF6 binding to a CRE-like probe. Competition with cold CRE-like probe (lane 2). Recombinant DREAM protein, alone or with repaglinide did not modify the retarded band (lanes 3 and 4, respectively). Recombinant DREAM did not bind to the probe (lane 5). Repaglinide alone did not affect ATF6 binding to the probe (lane 6). Migration of the free CRE-like probe (lane 7). Arrowhead, retarded band.



Supplemental Figure 12. Assessment of the fidelity of subcellular fractionation. Western blot analysis showing the fidelity of the subcellular fractionation. The nuclear markers, Lamin A/C, TBP and CREB, are absent in the cytosol. The cytosolic markers, Erk, PI3 kinase (p85 β) and tubulin, are excluded from the nuclear extract preparation.

Supplementary Table 1 Case information for human samples used in this study.

Code	Gender	Age	Phenotype	RN	YD	V
BCPA0056	M	75	C			
BCPA0076	M	49	C			
BCPA0177	F	58	C			
BCPA0260	F	55	C			
BCPA0281	M	41	C			
BCPA0079	M	61	HD	41	20	4
BCPA0112	F	53	HD	40	n.a.	2
BCPA0138	M	43	HD	49	n.a.	2
BCPA0324	M	55	HD	39	21	3
BCPA0336	F	62	HD	51	18	3
BCPA0439	M	72	HD	43	37	3

RN, major allele repeat number; YD, years of disease; V, Vonsattel grade; n.a. not available

Supplemental Table 2 List of genes downregulated in R6/2 striatum, whose expression is recovered in R6/2xDREAM^{+/-} striatum.

Supplemental Table 3 List of genes upregulated in R6/2 striatum, whose expression is recovered in R6/2xDREAM^{+/-} striatum.